JOC Article

Solution Conformations of Mycothiol Bimane, 1-D-GlcNAc-α-(1 → 1)-D-*myo*-Ins and 1-D-GlcNAc-α-(1 → 1)-L-*myo*-Ins

Janaki Mahadevan, Gillian M. Nicholas, and Carole A. Bewley*

Laboratory of Bioorganic Chemistry, National Institute of Diabetes and Digestive and Kidney Diseases, National Institutes of Health, Bethesda, Maryland 20892-0820

caroleb@intra.niddk.nih.gov

Received December 18, 2002

Mycothiol is an abundant small molecular weight thiol found only in actinomycetes, which include mycobacteria. Mycothiol biosynthetic and detoxification enzymes are novel and unique to actinomycetes, thereby representing potential antimycobacterial targets. To better guide inhibitor design, we have determined by NMR the solution conformations of mycothiol bimane (MSmB) and the pseudodisaccharide 1-D-GlcNAc-α-(1 → 1)-D-*myo*-Ins (D-GI), molecules that represent the natural substrates for the mycothiol-dependent detoxification enzyme mycothiol-*S*-conjugate amidase (MCA) and the mycothiol biosynthetic enzyme D-GlcNAc-α-(1 → 1)-D-*myo*-Ins deacetylase (AcGI deacetylase), respectively. Comparison of the mean structure of MSmB and the energy-minimized structures of two competitive spiroisoxazoline-containing MCA inhibitors shows striking similarities between these molecules in the region of the scissile amide bond of MSmB and provides structural evidence that those inhibitors are substrate mimics. Owing to our earlier finding that AcGI deacetylase will not deacetylate the unnatural isomer 1-D-GlcNAc-α-(1 → 1)-L-*myo*-Ins (L-GI), the solution conformation of L-GI was also determined. The interglycosidic bond angles for all three compounds are comparable. When considered together with the observation that a simplified cyclohexyl thioglycoside mycothiol analogue is a good substrate for MCA, it appears that the stereochemistry of the inositol ring is critical for deacetylase function, superseding the importance of the full complement of hydroxyl groups on the "nonreducing" ring.

Introduction

Low-molecular weight thiols play a fundamental role in protecting organisms from oxidative stress. Eukaryotes and Gram-negative bacteria employ glutathione for this purpose. Some actinomycetes, however, do not produce glutathione, but biosynthesize instead the compound 1-D-*myo*-inosityl 2-(*N*-acetyl-L-cysteinyl)amido-2-deoxy-α-D-glucopyranoside (**1**), commonly known as mycothiol (MSH).[1−3] All but one of the enzymes involved in the biosynthesis and reductive maintenance of mycothiol in *Mycobacterium smegmatis* and *Mycobacterium tuberculosis* have been described (Scheme 1).[4] These include the biosynthetic enzymes 1-D-GlcNAc-α-(1→1)-D-*myo*-Ins deacetylase (AcGI deacetylase),[5] a cysteinyl-transferase homologous to tRNA cysteinyl synthetases,[6] and an acetyl transferase.[7] The enzyme mycothione reductase catalyzes the reduction of the oxidized dimer of mycothiol, namely mycothione, to mycothiol.[8] In addition, the mycothiol-dependent detoxification enzyme, mycothiol-*S*-conjugate amidase (MCA), has been characterized from *M. tuberculosis* and *M. smegmatis*.[9,10] Like glutathione, mycothiol mediates detoxification in actinomycetes by seizing alkylating agents and other toxins through coupling to the cysteine sulfhydryl, after which MCA facilitates excretion of uric acid derivatives via cleavage of the scissile amide bond (Figure 1) of mycothiol-*S*-conjugates. Thus far, mycothiol-related enzymes that have been cloned and characterized represent enzymes from *M. tuberculosis* and *M. smegmatis*. Two of these enzymes in particular, namely MCA and AcGI deacetylase, are novel in that they cannot be placed into any known protein families at this time. Owing to the continuing need for new classes of antituberculars, interest in these enzymes as possible drug targets is rising.

We have been engaged in the identification of inhibitors to MCA and AcGI deacetylase, enzymes that display

* To whom correspondence should be addressed. Phone: 301-594-5187. Fax: 301-402-0008.

(1) Sakuda, S.; Zhou, Z.; Yamada, Y. *Biosci. Biotech. Biochem.* **1994**, *58*, 1347−1349.
(2) Spies, H. S.; Steenkamp, D. J. *Eur. J. Biochem.* **1994**, *224*, 203-213.
(3) Newton, G. L.; Bewley, C. A.; Dwyer, T. J.; Horn, R.; Aharonowitz, Y.; Cohen, G.; Davies, J.; Faulkner, D. J.; Fahey, R. C. *Eur. J. Biochem.* **1995**, *230*, 821−825.
(4) Reviewed in: Newton, G. L.; Fahey, R. C. *Arch. Microbiol.* **2002**, *178*, 388−394.
(5) Newton, G. L.; Av-Gay, Y.; Fahey, R. C. *J. Bacteriology* **2000**, *24*, 6958−6963.
(6) Sareen, D.; Steffek, M.; Newton, G. L.; Fahey, R. C. *Biochemistry* **2002**, *41*, 6885−6990.
(7) Koledin, T.; Newton, G. L.; Fahey, R. C. *Arch. Microbiol.* **2002**, *178*, 331−337.
(8) Patel, M. P.; Blanchard, J. S. *Biochemistry* **1999**, *38*, 11827−11833.
(9) Newton, G. L.; Av-Gay, Y.; Fahey, R. C. *Biochemistry* **2000**, *39*, 10739−10746.
(10) Nicholas, G. M.; Kovác, P.; Bewley, C. A. *J. Am. Chem. Soc.* **2002**, *124*, 3492−3493.

10.1021/jo026872w

 Published on Web 03/21/2003

SCHEME 1. Mycothiol Biosynthetic Scheme[a]

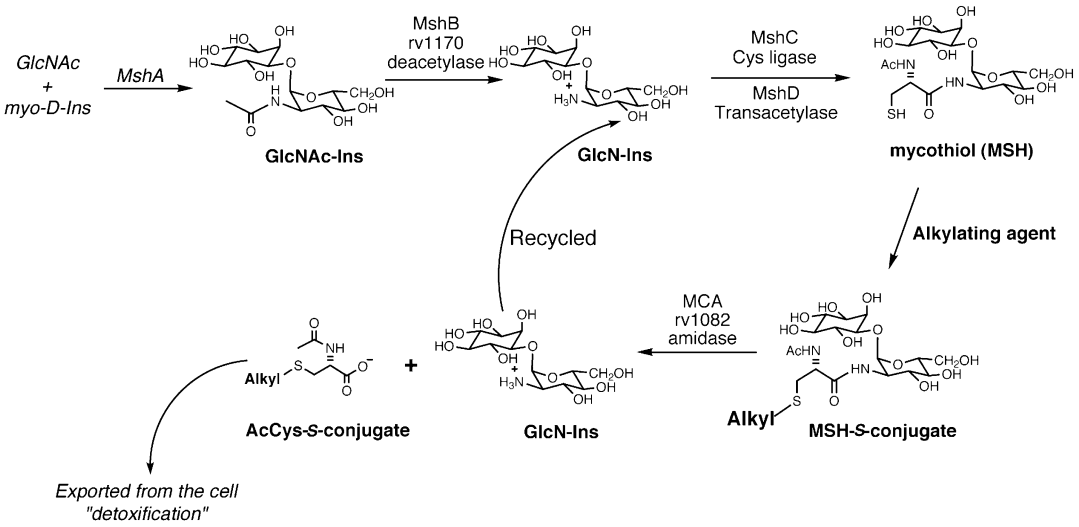

[a] With the exception of the first putative glycosyl transferase step carried out by MshA (denoted in italics), the enzymes involved in each step of MSH biosynthesis and MSH-facilitated detoxification have been described (refs 4−9). Note that the deacetylase MshB is also referred to in the literature as AcGI deacetylase and rv1170 as annotated in the *M. tuberculosis* genome. Similarly, MCA is referred to as rv1082.

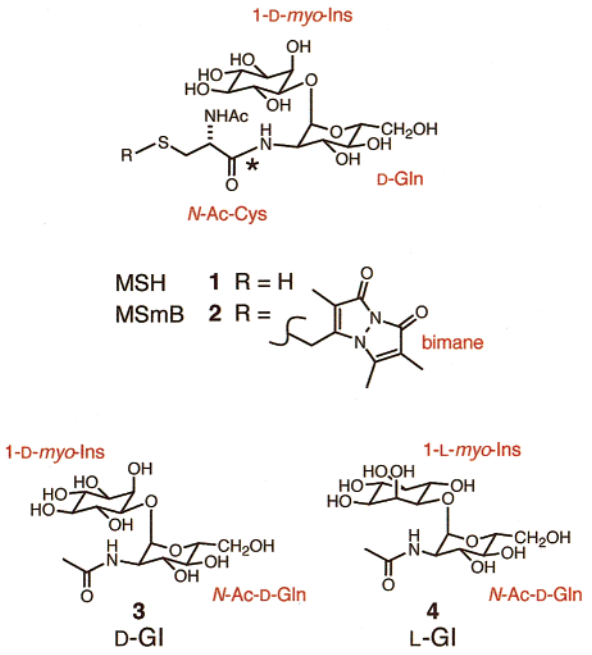

FIGURE 1. Structures of mycothiol (MSH, **1**), mycothiol bimane (MSmB, **2**), 1-D-GlcNAc-α-(1 → 1)-D-*myo*-Ins (D-GI, **3**), and 1-D-GlcNAc-α-(1 → 1)-L-*myo*-Ins (L-GI, **4**). The scissile amide bond in MSmB is denoted with an asterisk.

∼60% sequence homology to one another, and reported earlier several diverse classes of MCA inhibitors.[11−13] A comparison of the structures of those compounds strongly suggested that the detoxification enzyme MCA is a metalloprotein and that a competitive class of inhibitors featuring a bromotyrosine-derived spiroisoxazoline unit mimics the substrate mycothiol.[13] To better compare the conformations of substrate and inhibitor, as well as to guide inhibitor design, we have determined the solution conformations of mycothiol bimane (**2**, MSmB), an optimal substrate[9] for MCA, and 1-D-GlcNAc-α-(1 → 1)-D-*myo*-Ins (**3**, D-GI), the natural substrate of the biosynthetic enzyme AcGI deacetylase. Owing to our earlier finding that AcGI deacetylase will not deacetylate the unnatural isomer 1-D-GlcNAc-α-(1 → 1)-L-*myo*-Ins (**4**, L-GI),[14] we also determined the solution conformation of this compound. While the conformation of mycothiol bimane was determined on free substrate, we observe striking spatial similarities between the competitive spiroisoxazoline class of inhibitors and MSmB. This information should aid in the design and optimization of substrate-based synthetic inhibitors of MCA and AcGI deacetylase.

Results and Discussion

General Structure Determination. The solution conformations of **2**−**4** were determined by NMR using the program Xplor-NIH[15] employing distance and dihedral angle restraints, and for MSmB, $^{3}J_{CH}$ coupling restraints[16] as well. Two NMR samples (∼10 mM) were prepared for each compound by dissolving in either 99.9% D_2O or 10% D_2O in water, and the pH of each was adjusted to 6.5. Chemical shift assignments were made by interpretation of COSY and $^{1}H-^{13}C$ HSQC experiments, with t_1 set to observe either $^{1}J_{CH}$ or $^{2,3}J_{CH}$ couplings in the HSQC spectra, recorded on the D_2O samples. The exchangeable NH protons were then as-

(11) Nicholas, G. M.; Newton, G. L.; Fahey, R. C.; Bewley, C. A. *Org. Lett.* **2001**, *3*, 1543−1346.
(12) Nicholas, G. M.; Eckman, L. L.; Ray, S.; Hughes, R. O.; Pfefferkorn, J.; Barluenga, S.; Nicolaou, K. C.; Bewley, C. A. *Bioorg. Med. Chem. Lett.* **2002**, *12*, 2487−2490.
(13) Nicholas, G. M.; Eckman, L. L.; Newton, G. L.; Fahey, R. C.; Ray, S.; Bewley, C. A. *Bioorg. Med. Chem.* **2003**, *11*, 601−608.
(14) Nicholas, G. M.; Kovác, P.; Bewley, C. A. *Bioorg. Med. Chem.* **2003**, in press.
(15) Schwieters, C. D.; Kuszewski, J.; Tjandra, N.; Clore, G. M. *J. Magn. Reson.* **2003**, *160*, 66−74.
(16) Garrett, D. S.; Kuszewski, J.; Hancock, T. J.; Lodi, P. J.; Vuister, G. W.; Gronenborn, A. M.; Clore, G. M. *J. Magn. Reson. B*, **1994**, *104*, 99−103.

TABLE 1. Coupling Constants and NOE Intensities for D-GI (3)

residue		*J* (Hz)	NOE (intensity[a])
N-acetyl-1-α-D-glucosamine	1	d 3.5	1′ (s), 2′ (m), 6′ (m), 2 (m), 3 (m), 4 (w), 5 (w)
	2	dd 10, 3.5	1 (m), 4 (m)
	3	t 10	1 (m), 4 (m)
	4	t 10	1 (w), 2 (m), 3 (m), 5 (m)
	5	m	2′ (w), 1 (w), 4 (m)
	6a	m	
	6b	m	
	HN	d 9	1 (m), CH_3 (s)
	CO		
	CH_3	s	
1-D-*myo*-inositol	1′	dd 10, 3	1 (s), 2′ (m), 6′ (m)
	2′	t 3	1 (m), 5 (w), 1′ (m), 3′ (m), 4′ (m), 5′ (w), 6′ (m)
	3′	dd 10, 3	2′ (m), 4′ (m), 5′ (m)
	4′	t 10	2′ (m), 3′ (m)
	5′	t 10	2′ (m), 3′ (m)
	6′	t 10	1 (m), 1′ (m), 2′ (m)

[a] The letters s, m, and w refer to strong, medium, and weak intensities. See the Experimental Section for distances used in structure calculations.

TABLE 2. Coupling Constants and NOE Intensities for L-GI (4)

residue		*J* (Hz)	NOE (intensity[a])
N-acetyl-1-α-D-glucosamine	1	d 3.5	1′ (s), 2′ (m), 6′ (w), 2 (m), 3 (m)
	2	dd 10, 3.5	1 (m), 3 (m), 4 (m)
	3	t 10	2 (m), 4 (m)
	4	t 10	2 (m), 3 (m)
	5	m	1′ (m), 6′ (w)
	6a	m	
	6b	m	
	HN	d 9	1 (m), CH_3 (s)
	CO		
	CH_3	s	
1-L-*myo*-inositol	1′	dd 10, 3	1 (s), 5 (m), 2′ (m), 3′ (m), 5′ (m), 6′ (m)
	2′	t 3	1 (m), 1′ (m), 3′ (m)
	3′	dd 10, 3	1′ (m), 2′ (m), 4′ (m), 5′ (m)
	4′	t 10	2′ (m), 5′ (m), 6′ (m)
	5′	t 10	1′ (m), 3′ (m), 4′ (m), 6′ (m)
	6′	t 10	1 (m), 5 (w), 1′ (m), 4′ (m), 5′ (m)

[a] The letters s, m, and w refer to strong, medium, and weak intensities. See the Experimental Section for distances used in structure calculations.

signed from the1D ^{1}H NMR spectra recorded on the water samples. Full assignments are presented in Tables 1−3. Under the conditions used, no exchangeable hydroxyl protons were observed for any of the compounds in either sample. Distance restraints were obtained for each compound from a series of NOESY and ROESY spectra recorded with mixing times of 150 ms, 400 ms, and 1 s for the NOESY experiments and 25, 45, and 110 ms for the ROESY experiments. Distance restraints were then binned into strong, medium, and weak restraints relative to cross-peak volumes for geminal proton pairs (see the Experimental Section for details). Torsion angle restraints were derived from $^3J_{HH}$ values measured at 800 MHz on each sample and were consistent with a chair conformation for the cyclitol and pyranose rings in all three compounds. Thus, the topology files included standard intracyclitol and intrasugar restraints for bonds, angles, and impropers to maintain correct geometry. $^3J_{CH}$ values describing the interglycosidic bond were derived from 2D HSQMBC experiments[17] recorded on the D_2O samples.

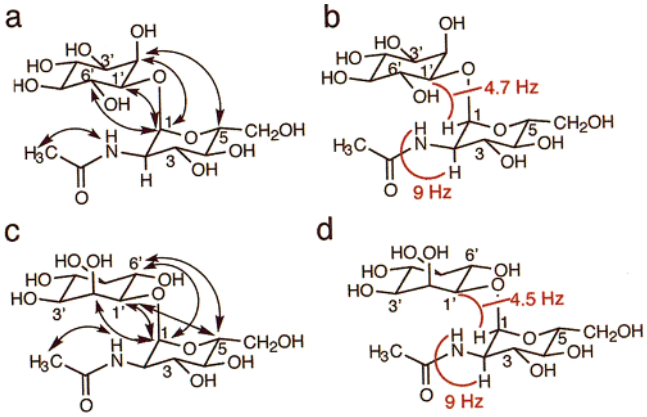

FIGURE 2. Key interresidue NOEs and coupling constants implemented as distance and dihedral angle restraints for (a, b) D-GI (**2**), and (c, d) L-GI (**3**).

Conformation of D-GI (3). The solution conformation of D-GI was calculated using a total of 24 distance restraints, 20 of which correspond to intraresidue NOEs and 4 to interresidue NOEs, along with five dihedral angle restraints describing the conformation of the *N*-acetyl group and the glycosidic bond. (These dihedral angle restraints are in addition to those of the topology files described earlier.) Key interresidue NOEs observed in the NOESY and ROESY spectra of D-GI are listed in Table 1 and illustrated in Figure 2a and include NOEs between H1 of *N*-Ac-Gln and H1′, H2′, and H6′ of 1-*myo*-D-Ins, and H5 and H2′. A $^3J_{HH}$ value of 9 Hz observed in a NOESY echo spectrum of the 10% D_2O sample of D-GI indicated trans geometry between HN and H2 and is consistent with the observed medium strength NOE between these two atoms. In addition, the strong NOE between HN and the CH_3 protons indicates a trans amide bond. Thus, four dihedral angle restraints were introduced to maintain this observed geometry.

In terms of additional dihedral angle restraints, a $^3J_{CH}$ value of 4.7 ± 0.5 Hz was measured in an HSQMBC spectrum for the interglycosidic bond H1−C1−O1′−C1′, yielding possible dihedral angles of approximately ±25° or ±140° for this bond. However, an interglycosidic bond of ±140° is unattainable in compound **3** due to steric clash. Thus, in the initial structure calculations, the H1−C1−O1′−C1′ dihedral angle was defined as 0° ± 55° to cover both possibilities. For structures calculated with these values, NOE violations were consistently observed for structures bearing positive glycosidic bond angles; thus the glycosidic bond was subsequently restrained to −30° ± 30°. Superpositions of a family of 40 structures with no NOE or dihedral angle violations greater than 0.1 Å or 5°, respectively, are shown in Figure 3a for D-GI. The root-mean-square deviation (rmsd) for all heavy atoms of this family of structures is 0.21 Å. The restrained, regularized mean structure is shown in a ball-and-stick representation in Figure 3b. Respective Φ (H1−C1−O1′−C1′) and Ψ (C1−O1′−C1′−H1′) values of −23°

(17) Williamson, R. T.; Márquez, B. L.; Gerwick, W. H.; Kövér, K. E. *Magn. Reson. Chem.* **2000**, *38*, 265−273.

TABLE 3. Coupling Constants and NOE Intensities for MSmB (4)

residue	atom no.	atom type	*J* (Hz)	NOE (intensity[a])
N-acetyl-L-cysteine	1	CO		
	2	Cα	m	3a (s), 3b (s), 8a (vw), 8b (w), 5 (w), 9 (vw), 7 (m)
	3	C*β*	dd 14, 8.5	7 (m), 3b (s), 2 (s), 8b (w)
			dd 14, 4.5	7 (m), 3a (s), 2 (s), 8a (w), 8b (vw)
	4	CO		
	5	CH_3	s	6″ (w), 2 (w)
	HN	HN	br d 4.5	2 (w), 5 (s)
bimane	1	CO		
	2	C		
	3	C		
	4	C		
	5	C		
	6	CO		
	7	CH_3	s	2 (m), 8a (w), 8b (w), 3a (m), 3b (m)
	8a	CH_2	d 15	7 (w), 9 (w), 3b (vw), 2 (vw)
	8b	CH_2	d 15	7 (w), 9 (w), 3a (w), 3b (w), 2 (w)
	9	CH_3	s	2 (vw), 8a (w), 8b (w)
	10	CH_3	s	
α-D-glucosamine	1′	CH	d 3.5	1″ (s), 2″ (m), 6″ (m), 2′ (s)
	2′	CH	dd 10, 3.5	1′ (m), 4′ (m)
	3′	CH	t 10	4′ (m)
	4′	CH	t 10	2′ (m), 3′ (m), 5′ (m)
	5′	CH	m	1″ (w), 2″ (s), 4′ (m)
	6a′	CH_2	m	
	6b′	CH_2	m	
	H′N	HN	d 9	2 (s), 1′ (m)
1-D-*myo*-inositol	1″	CH	dd 10, 3	1′ (s), 5′ (w), 2″ (m)
	2″	CH	t 3	1′ (m), 5′ (s), 1″ (m), 3″ (m), 4″ (m)
	3″	CH	dd 10, 3	2″ (m)
	4″	CH	t 10	2″ (m), 5″ (m)
	5″	CH	t 10	4″ (m), 6″ (m)
	6″	CH	t 10	1′ (m), 5″ (m), 5 (w)

[a] The letters s, m, and w refer to strong, medium, and weak intensities. See the Experimental Section for distances used in structure calculations.

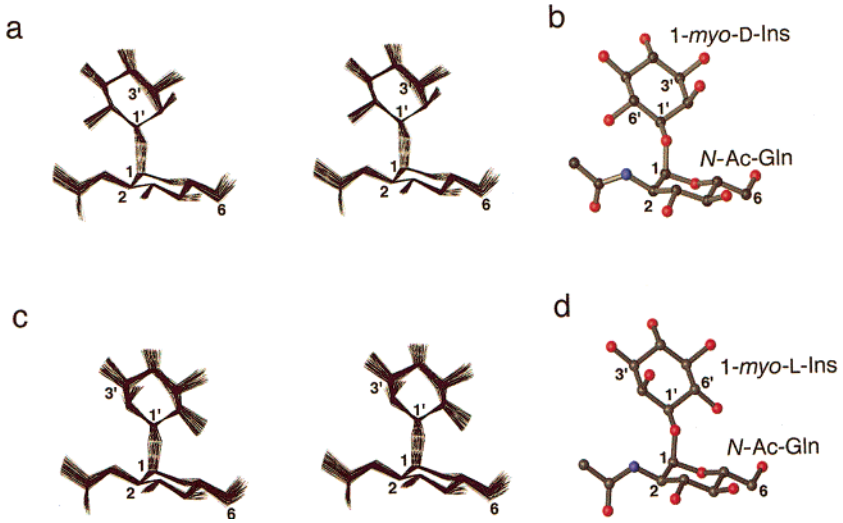

FIGURE 3. Superpositions and restrained, regularized mean structures for (a, b) D-GI (**2**) and (c, d) L-GI (**3**). Superpositions comprise a family of 40 structures with no NOE or dihedral angle violations greater than 0.1 Å or 5° best fitted to all heavy atoms of the pseudodisaccharide. The restrained, regularized mean structures (b, d) appear as ball-and-stick representations with carbon atoms colored gray, oxygen atoms colored red, and nitrogen atoms colored blue. Figures were generated using the programs VMD-XPLOR[30] (for the superpositions) and MolMol[31] (for the mean structures).

± 9° and 9° ± 6° orient the two rings almost perpendicular to one another, with H6′ of 1-*myo*-D-Ins situated above the scissile amide bond.

Conformation of the Unnatural Isomer L-GI (4). The solution conformation of L-GI was calculated on the basis of 23 experimental distance restraints where 18 corresponded to intracyclitol or intrapyranose NOEs and the remaining five to interresidue NOEs, along with five torsion angle restraints. In Figure 2c, interresidue NOEs are shown schematically and include correlations between the anomeric proton of *N*-Ac-Gln and H1′, H2′ and H6′ of 1-L-*myo*-Ins, while H5 showed a weak NOE to H6′, the regio-equivalent of H2′ in 1-*myo*-D-Ins, and to H1′. This last NOE was not observed for D-GI suggesting a

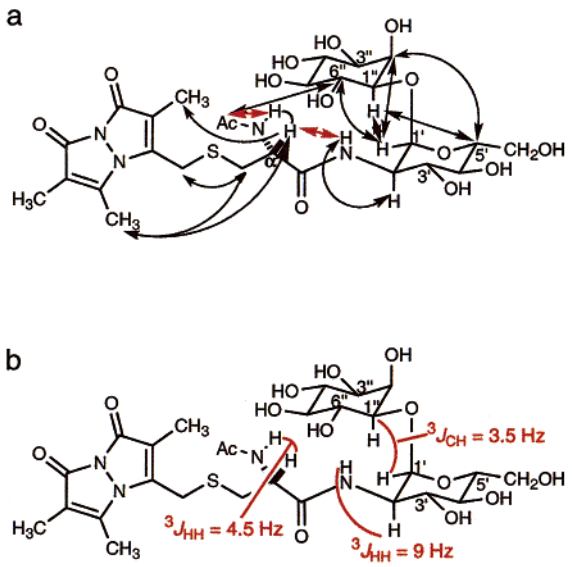

FIGURE 4. Key interresidue NOEs and coupling constants implemented as distance and dihedral angle restraints for MSmB (**1**), shown in (a) and (b), respectively. In **4a**, key strong NOEs are indicated by red arrows.

subtle difference in relative orientation between the Gln and Ins rings of D- and L-GI. Consistent with this pattern of NOEs, a slightly smaller value of 4.4 ± 0.5 Hz was observed in the HSQMBC spectrum for the H1−C1−O1′−C1′ dihedral angle. However, the dihedral angle restraints were introduced in the calculations of L-GI in an identical fashion as described above for D-GI. Best fitting of a family of 40 structures (Figure 3c) of L-GI, again with no respective NOE or dihedral angle violations greater than 0.1 Å or 5°, gives an rmsd of 0.25 Å. Superpositions of that family are shown in Figure 3c, and the restrained, regularized mean structure is shown in Figure 3d. Overall, the solution conformations of the two isomers are very similar to one another with L-GI displaying glycosidic Φ and Ψ values of −25° ± 10° and 4° ± 9°.

Conformation of Mycothiol Bimane (2). The solution structure of mycothiol bimane is based on a total of 27 distance restraints and 12 dihedral angle restraints. The intraresidue distance restraints derive from six intra-glucosamine, five intra-inositol, and three intra-cysteine NOEs. Although intra-bimane NOEs were observed, it was not necessary to include them in the calculations because 18 planarity restraints were introduced to maintain correct planar geometry for the bimane rings. Interresidue distance restraints were introduced on the basis of five NOEs observed between Gln and 1-*myo*-D-Ins, one NOE between Ac-Cys and Gln, one NOE between Ac-Cys and 1-*myo*-D-Ins, and five NOEs between Ac-Cys and the bimane moiety (Figure 4a). The ^3J(H′N−H2′) value of 9 Hz observed for MSmB is identical to that measured for equivalent atoms in D-GI, and the pattern of NOEs observed between Gln and 1-*myo*-D-Ins in MSmB is similar to that observed for D-GI (Figs 2a, 4a). However, a slightly smaller ^3J(C1″−H1′) value of 3.5 Hz was observed for MSmB and is consistent with the observed Φ and Ψ values of −54° ± 12° and −2° ± 20°.[18,19]

In terms of amide bond conformations, the large ^3J(H′N−H2′) value of 9.0 Hz and the relatively weak NOE observed between this pair of resonances, together with the strong NOE observed between H′N and Hα of *N*-Ac-Cys, are indicative of an all-trans conformation from HN of Gln to Hα of *N*-Ac-Cys. Indeed, initial structures converged to an all-trans conformation for these atoms, allowing corresponding dihedral angles restraints to be introduced. For the *N*-Ac-Cys residue, a $^3J_{HH}$ value of 4.5 Hz for Hα to HN together with the weak NOE observed for this pair is consistent with the observed dihedral angle value of −150°. As seen in Figure 4b, several NOEs were observed between resonances belonging to *N*-Ac-Cys and the bimane moiety. However, stereospecific assignments could not be made for the methylene protons (H3a/H3b and H8a/H8b) on the basis of NOEs or coupling constants indicating rotamer averaging. The large range of orientations occupied by the bimane moiety is apparent in the superpositions of MSmB shown in Figure 5a and is reflected in the rather large rms deviation of 1.41 Å for all heavy atoms of MSmB. In comparison, an rmsd of 0.52 Å is observed when the bimane moiety is excluded from the fitting.

Comparison of MSmB and Spiroisoxazoline Inhibitors of MCA. Earlier, we identified 13 natural product inhibitors of the detoxification enzyme mycothiol-*S*-conjugate amidase that represented six different structural classes.[11,13] Kinetics and inhibition studies on compounds representative of four of those classes showed that spiroisoxazoline- and bromophenyl oximinoamide-containing natural products competed directly with the optimal substrate MSmB for MCA activity. Moreover, comparisons of the structures of the natural product inhibitors strongly suggested that MCA is a metalloenzyme[20] and that both the competitive and noncompetitive inhibitors may act by either chelating structural or catalytic metal ions in MCA, displacing the substrate from the active site, or both. As seen in Figure 6a, examples of the spiroisoxazolines include pseudoceratine[21] (**5**) and compound **6**,[11] while compounds **7**[22] and **8**[11] are representative of the bromophenyl oximinoamides.

To further compare the conformations of free MSmB with the competitive inhibitors, we best fit the central amide bond of the energy minimized structure of the competitive inhibitors **5** and **6** (Figure 6c) with the scissile amide bond of the acetate group of the solution structure of MSmB (Figure 6b). Although the solution conformation of MSmB determined here is of the free substrate, there are striking similarities between MSmB and the inhibitors. In particular, to the carboxy side of the amide in inhibitor **6** and MSmB, the N and O atoms of the oxazole ring and the C-1 hydroxyl align well with the N and O atoms of the acetyl amido group of *N*-acetyl-Cys. In addition to our earlier kinetics studies, these structural similarities provide supporting evidence that this class

(18) Mulloy, B.; Frenkiel, T. A.; Davies, D. B. *Carbohydrate Res.* **1988**, *184*, 39−46.
(19) Tvaroska, I.; Hricovíni, M.; Petráková, E. *Carbohydrate Res.* **1989**, *189*, 359−362.
(20) Unpublished data in our laboratory demonstrates that inclusion of EDTA in MCA solutions renders MCA inactive, and prolonged storage of MCA in buffers lacking Zn^{2+} results in greatly diminished amidase activity providing further evidence that MCA is a metalloenzyme.
(21) Benharref, A.; Pais, M. *J. Nat. Prod.* **1996**, *59*, 177.
(22) Litaudon, M.; Guyot, M. *Tetrahedron Lett.* **1986**, *27*, 4455.

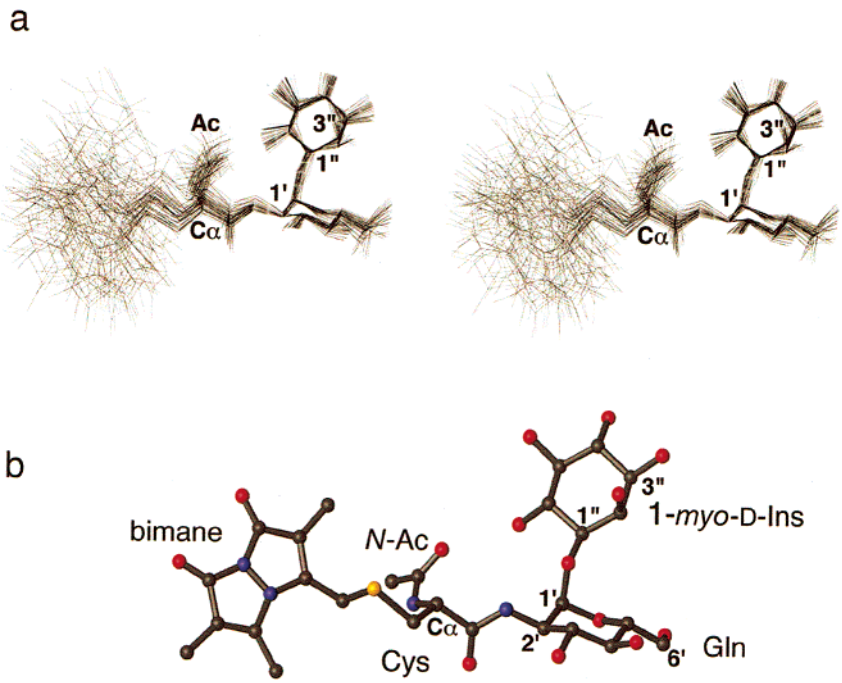

FIGURE 5. (a) Superpositions and (b) the mean structure of MSmB. Superpositions comprise a family of 40 structures with no NOE or dihedral angle violations greater than 0.1 Å or 5° best fitted to the mycothiol portion of MSmB, that is, discluding the bimane moiety. The mean structure is drawn in a ball-and-stick representation with carbon atoms colored gray, oxygen atoms colored red, nitrogen atoms colored blue, and the sulfur atom colored gold.

of spiroisoxazoline natural products are structural mimics for MSmB. For MSmB and the detoxification enzyme MCA, our earlier findings demonstrated that the presence of the rigid spiroisoxazoline ring, relative to the more flexible bromophenyl oximinoamides (**7** and **8**), yields a more potent inhibitor. In light of these findings, it is interesting to note that several examples of synthetic oxazole- and thiazole-containing compounds designed to inhibit other proteinases or deacetylases have been published recently.[23] In those and related studies, the impetus for inclusion of an oxazole moiety stems from its likely metal-chelating properties.

Concluding Remarks. We have determined the solution conformations of D-GI (**3**), L-GI (**4**) and MSmB (**2**) by NMR spectroscopy and simulated annealing. For each molecule, the interglycosidic bond angles are comparable yielding similar conformations for the pseudo-disaccharide portion of the substrates. Recently we domonstrated that the mycothiol analogue cyclohexyl thioglycoside served as a good substrate for MCA,[24] whereas the unnatural isomer L-GI could not be deacetylated by the biosynthetic enzyme AcGI deacetylase even at mM concentrations.[14] The stereochemistry at C2 and C6 of *myo*-inositol distinguishes the D- and L-isomers. Together with the solution conformations determined here, these cumulative findings suggest that the stereochemistry of the inositol ring is critical for enzyme function, superseding the importance of the full complement of hydroxyl groups on the "nonreducing" ring.

Experimental Section

General Methods. Synthetic samples of MSmB, D-GI, and L-GI were prepared as described in refs 10 and 14. All NMR experiments were recorded at 27 °C on Bruker DMX500, DMX600, DMX750, and DRX800 spectrometers equipped with *x*,*y*,*z*-shielded gradient triple resonance probes or cryoprobes. Shigemi tubes were used for all samples. In general, spectra were recorded with spectral widths of 8.0 ppm for D_2O samples and 10 ppm for water samples, with spectral widths of 1024 complex points in F2 and either 120 or 200 ppm and 256 complex points in F1. The only exception was the HSQMBC experiments in which the number of points was increased 2-fold in both dimensions. For scalar coupled experiments, the carrier was set on water, and for dipolar coupling experiments, the carrier was set outside of the spectral region containing proton resonances. Spectra were processed with the NMRPipe package[25] and spectra analyzed using the program PIPP.[26] The pH for each 300 μL sample was adjusted with either 0.1 M NaOD or DCl.

Structure Calculations. Initial energy-minimized coordinates for D-GI, L-GI, and MSmB were generated using the program Chem3D followed by a second round of minimization using the program Xplor-NIH[15] (http://nmr.cit.nih.gov/xplor-nih/). Topology and parameter files were then generated using the program XPLO2D[27] (http://alpha2.bmc.uu.se/~gerard/manuals/), and dihedral angle values were checked by hand to ensure removal of restraints for rotatable bonds. All structures were calculated on the basis of distance, dihedral

(23) Several examples include: (a) Kline T.; Andersen N. H.; Harwood E. A.; Bowman, J.; Malanda, A.; Endsley, S., Erwin, A. L.; Doyle, M.; Fong, S.; Harris, A. L.; Mendelsohn, B.; Mdluli, K.; Raetz, C. R.; Stover, C. K.; Witte, P. R.; Yabannavar, A.; Zhu, S. *J. Med. Chem.* **2002**, *45*, 3112−3129. (b) Scozzafava, A.; Supuran, C. T. *Bioorg. Med. Chem. Lett.* **2002**, *12*, 2667−2672. (c) Pirrung, M. C.; Tumey, L. N.; Raetz, C. R.; Jackman, J. E.; Snehalatha, K.; McClerren, A. L.; Fierke, C. A.; Gantt, S. L.; Rusche, K. M. *J. Biol. Chem.* **2000**, *275*, 11002−11009.

(24) Knapp, S.; Gonzalez, S.; Myers, D. S.; Eckman, L. L.; Bewley, C. A. *Org. Lett.* **2002**, *4*, 4337−4339.

(25) Delaglio, F.; Grzesiek, S.; Vuister, G. W.; Zhu, G.; Pfeifer, J.; Bax, A. *J. Biomol. NMR* **1995**, *6*, 277−293.

(26) Garrett, D. S.; Powers, R.; Gronenborn, A. M.; Clore, G. M. *J. Magn. Reson.* **1991**, *95*, 214−220.

(27) Kleywegt, G. J. Dictionaries for Heteros. CCP4/ESF-EACBM Newsletter on Protein Crystallography 31, June 1995; pp 45−50.

TABLE 4. Structural Statistics

	D-GI	L-GI	MSmB
distance restraints			
intraresidue NOEs	20	18	14
interresidue NOEs			
Gln-Ins	4	5	5
Gln-*N*-Ac-Cys			1
Ins-*N*-Ac-Cys			1
N-Ac-Cys-bimane			6
torsion angle restraints[a]	5	5	12
rms deviations from distance restraints[b]	0.011 (±0.028)	0.000 (±0.000)	0.012 (±0.011)
rms deviations from dihedral angle restraints[b]	0.016 (±0.036)	0.005 (±0.002)	0.166 (±0.001)
rms deviations from coupling restraints[c]			0.628 (±0.015)
coordinate precision (Å)[d]			
all heavy atoms	0.21 (±0.07)	0.25 (±0.08)	1.41 (±0.29)
N-Ac-Cys-Gln-Ins			0.53 (±0.16)

[a] These torsion angle restraints comprise those derived from experimental *J* couplings for interresidue linkages and are in addition to standard angle and improper torsions included to maintain chair conformations consistent with intraresidue NOEs for the cyclitol and pyranose rings. [b] None of the final set of 40 structures exhibited distance violations greater than 0.1 Å or dihedral angle violations greater than 5° [c] Experimental *J* couplings were introduced in the form of coupling constant restraints for the peptide bonds of MSmB. None of the final set of 40 structures exhibited coupling constant violations greater than 0.6 Hz. [d] The precision of the coordinates is defined as the average rms difference between the 40 individual structures and the mean coordinate positions for the respective mean structures (for D-GI, D-GI, and MSmB) obtained by best fitting to all heavy atoms unless otherwise specified.

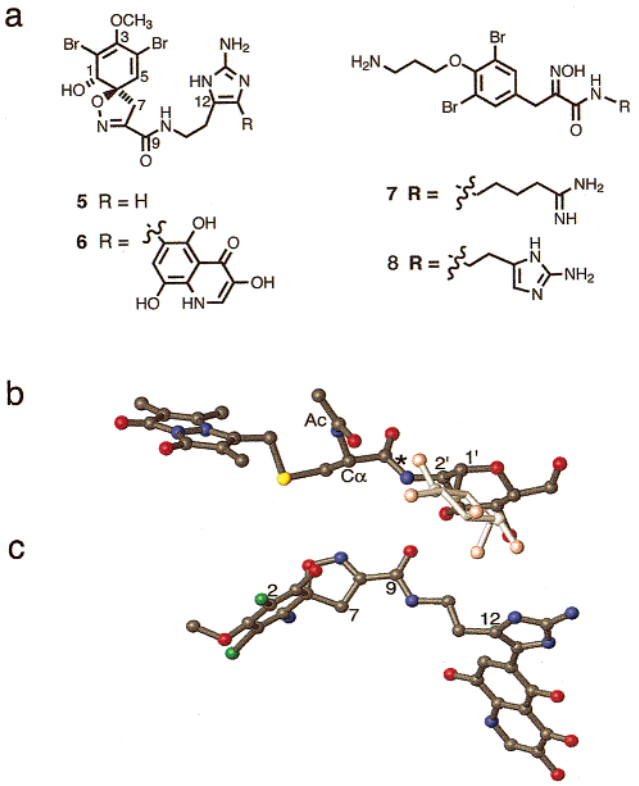

FIGURE 6. Comparison of bromotyrosine-derived natural product inhibitors of MCA with MSmB. (a) Chemical structures of pseudoceratine (**5**),[21] the uranidine-containing spiroisoxazoline **6**,[11] and bromophenyl oximinoamide inhibitors **7**[22] and **8**.[11] (b) Solution structure of MSmB and (c) an energy-minimized structure of inhibitor **6**. For (b) and (c), the structures were superimposed by overlaying, respectively, the scissile amide bond and the N and O atoms of the aceto amido group of MSmB (**1**) with the central amide and the N and O atoms of the oxazole ring and the C-1 hydroxyl of inhibitor **5**, using the program GRASP.[32] Atoms are colored as in Figures 3 and 5, with bromine atoms colored green. For clarity, the carbon and oxygen atoms of 1-*myo*-D-Ins are colored white and pink, respectively.

angle, and in the case of MSmB $^3J_{CH}$ coupling constant restraints (summarized in Table 4). The interglycosidic bond angle restraints derived from experimental $^3J_{CH}$ values, and calculated structures were compared with those predicted for Karplus and modified Karplus expressions and found to be consistent with each.[18,19] Interproton distance restraints derived from NOE spectra were grouped into three ranges corresponding to strong (1.8−3.0 Å), medium (1.8−4.0 Å), and weak (1.8−5.0 Å) NOEs. An additional 0.5 Å was added to the upper bound for NOEs involving methyl groups and 0.2 Å for NOEs involving NHs.[28] Distances involving nonstereospecifically assigned protons were represented by a $(\Sigma r^{-6})^{-1/6}$ sum.[29] The final values for the force constants employed for the various terms in the target function are as follows: 1000 kcal mol^{-1} Å^{-1} for bond lengths, 500 kcal mol^{-1} rad^{-1} for angles and improper torsions (which serve to maintain chirality and planarity), 4 kcal mol^{-1} Å^{-1} for the quartic van der Waals repulsion term (with the van der Waals radius scale factor set to 0.8), 30 kcal mol^{-1} Å^{-1} for the experimental distance restraints, 200 kcal mol^{-1} rad^{-1} for the torsion angle restraints, and 1.0 kcal mol^{-1} Hz^{-1} for the ^3J coupling constant restraints. Intraresidue and interresidue restraints are included for **2**−**4**, and the structural statistics for each are summarized in Table 4.

Acknowledgment. We thank Marius Clore, Charles Schweiters, and Thomas Williamson for helpful discussions. This work was supported in part by the Intramural AIDS Targeted Antiviral Program of the Office of the Director (C.A.B.).

Supporting Information Available: Tables of complete ^{1}H and ^{13}C NMR assignments in water for compounds **2**−**4** and copies of ROESY and HSQMBC spectra with expansions of the anomeric region for MSmB. This material is available free of charge via the Internet at http://pubs.acs.org.

JO026872W

(28) Clore, G. M.; Gronenborn, A. M.; Nilges, M.; Ryan, C. A. *Biochemistry* **1987**, *26*, 8012−8023.
(29) Nilges, M. *Proteins* **1993**, *17*, 297−309.
(30) Schweiters, C. D.; Clore, G. M. *J. Magn. Reson.* **2001**, *149*, 239−244.
(31) Koradi, R.; Billeter, M.; Wuthrich, K. *J. Mol. Graphics* **1996**, *14*, 51−55.
(32) Nichols, A.; Sharp, K. A.; Honig, B. *Proteins Struct. Func. Gen.* **1991**, *11*, 281−296.